Infra-red signature reduction study on a small-scale jet engine

J. Dix, A.J. Saddington, K. Knowles and M.A. Richardson
Department of Aerospace, Power and Sensors,
Cranfield University,
RMCS, Shrivenham,
Swindon, UK

ABSTRACT

This paper presents infra-red signature data for a small-scale, low pressure ratio turbojet engine typical of that used in unmanned air vehicle applications. The aim of the study was to test a number of different convergent nozzle designs concentrating on those with trailing edge modifications. The engine used in the tests has a single stage centrifugal compressor and radial inflow turbine and is designed to produce approximately 150N of thrust at 103,500rpm using liquid propane fuel. The test rig consisted of a calibrated thrust stand whilst the engine was controlled through an electronic engine control unit and laptop PC. The jet plume was visualised using an infra-red spectroradiometer which yielded qualitative data across the infra-red spectrum. Simultaneous measurements were also made of the engine thrust. A Pitot probe was used to take pressure readings across different sections of the exhaust flow. Analysis of the infra-red signature of the engine exhaust plume and any thrust penalty yielded a performance comparison for each of the nozzles tested. Correlation of engine thrust with engine rpm showed that, within the accuracy of the measurements, there was no significant thrust penalty associated with the notched nozzles. Infra-red imagery of the plain and 60° notched nozzles indicated that the latter reduced the length of the hottest part of the exhaust plume by approximately 33%. The spectroradiometer data shows a significant reduction in spectral radiance for the CO_2 wavelength of approximately 4·3μm when the notched nozzles are used. The 60° notched nozzle appeared to perform best in reducing the spectral radiance at this wavelength. Centreline total pressure measurements in the exhaust plume correlated well with the infra-red imagery in that a potential core length reduction of up to 30% could be achieved using the 60° notched nozzle. Total pressure contours recorded 20mm (0·43*D*) downstream of the nozzle exit plane suggest that the notched nozzles are promoting increased mixing through radial spreading of the jet possibly associated with increased streamwise vorticity (although the latter could not be confirmed). There were also signs that the jet plumes being investigated were swirling.

1.0 INTRODUCTION

The use of infra-red guided missiles remains a continued threat to manned and unmanned aircraft. Typically, infra-red seekers have been designed to detect hot engine parts and exhaust gas emissions. The exhaust gas signature comprises primarily the emissions from H_2O (at approximately 2·7μm wavelength) and CO_2 (at approximately 4·3μm wavelength) with the contemporary seeker usually concentrating on the wavelength spread about the CO_2 component. Reducing the infra-red signature will enhance the survivability of an aircraft in a hostile environment. For example a single F-117A, flying a single sortie and dropping one bomb, is claimed to be able to achieve the same operational effectiveness as 95 sorties and 190 bombs as used with conventional aircraft in the Vietnam War[1]. Additionally, a reduction in infra-red signature will enable the power requirements of countermeasure devices such as DIRCM (directed infra-red countermeasure) to be reduced.

Exhaust plume infra-red signature may be reduced, for example, through the use of a high bypass ratio engine, changes in nozzle design and shielding[1]. In the case of nozzle design modifications, the aim is to promote more rapid mixing of the exhaust plume with the surrounding ambient air to reduce the infra-red signature. The generation of stream-wise vortices has been shown to be beneficial[2] and schemes have been investigated using vortex generators, tabs[3] and other intrusive devices. Nozzle lip or trailing edge modifications have been shown in previous studies to have significant effect on jet development[4, 5]. For example, triangular notches in the nozzle lip generate strong stream-wise vortices and distort the jet cross-section[6]. A similar effect has been shown for castellated nozzles, but only at underexpanded conditions[7]. Most of these previous studies, however, have concentrated on the mixing enhancement rather than direct measurement of the infra-red signature.

A version of this paper was presented at the 2004 RAeS Aerospace Aerodynamics Research Conference

https://doi.org/10.1017/S0001924000000580 Published online by Cambridge University Press

As well as considering the infra-red signature, this study also considers how the nozzle modifications affect the thrust produced by the engine. When comparing infra-red signatures it is important to do this at constant levels of thrust since this is what determines the performance of the air vehicle. If the efficiency of the low infra-red nozzle forces the engine to run faster and/or hotter then much of the benefit of the nozzle may be lost.

This paper presents an experimental study of the effect of modifications to a baseline convergent nozzle on the infra-red signature of a low-cost commercial turbo-jet engine suitable for unmanned air vehicle applications.

2.0 AIMS AND OBJECTIVES

The aim of the project is to lower the infra-red signature of the jet engine under consideration through the use of nozzle modifications without incurring a large thrust penalty. It is important to try to maintain the level of thrust produced by the engine otherwise a retro fit would not be possible.

The objectives of the research are to:

- test six different convergent nozzle designs over a range of engine thrust levels (speeds);
- take spectroradiometer measurements of the exhaust plume for each nozzle design;
- simultaneously record the engine thrust;
- take centreline and cross-plane Pitot probe measurements in the exhaust plume.

3.0 METHODOLOGY

After assessing previous work it was decided that nozzles with four triangular notches would be tested. Four convergent nozzles with a 47mm exit diameter, D were made from 0·5mm thick stainless steel sheet with sections of 25°, 35°, 45° and 60° included angle removed at four equal points around the nozzle exit perimeter. The exit perimeter was kept constant (apart from the plain nozzle) by varying the depth of each triangular notch, taking the 45° nozzle as the reference with 20mm deep cut outs. The perimeter was kept constant to try and reduce the number of variables during the testing. A fifth nozzle was left as a truncated cone to act as the control nozzle and a sixth nozzle was made with four equally-spaced triangular tabs each with a base and height of 10mm. The tabs were mounted perpendicular to the flow pointing towards the centre of the nozzle exit. All the nozzles are illustrated in Fig. 1. Each nozzle was held by a ring of six nuts and bolts and sealed to the back of the engine with silicone sealant.

The test set-up was based around the James Engineering Turbines Cobra turbo-jet engine, mounted on a linear guide, which in turn was bolted to a large aluminium frame (see Fig. 2). The engine has a centrifugal compressor, radial inflow turbine and reverse flow annular combustor. It has a total loss lubrication system, using compressor bleed air to pressurise the oil tank (foreground of Fig. 2). The engine has the specifications described in Table 1[8]. The notched nozzles were mounted on the engine such that the notches were orientated along the x and y axes shown in Fig. 2.

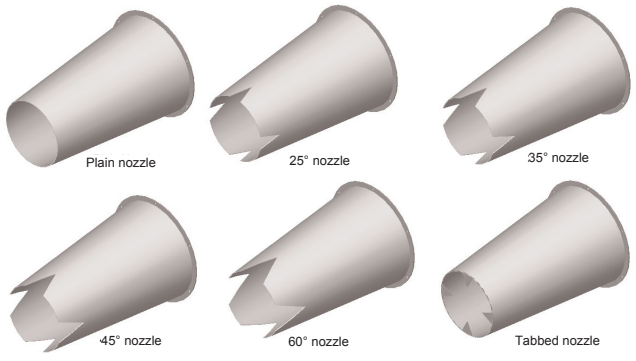


Figure 1. The nozzle designs used in the test programme.

Table 1
Basic specifications of the James turbo-jet engine

Mass	3·1kg
Diameter	0·17m
Fuel	Liquid propane
Pressure ratio	2·9:1
Mass flow rate	0·3kgs^{-1} (air) (max. speed)
Thrust	150N @ 103,500rpm (max speed)
	6N @ 30,000rpm (idle)

3.1 Thrust measurements

A load cell was used to measure engine thrust. It was mounted on to the test stand in such a way as to allow the engine to slide along the linear guide and push against the load cell. The load cell used was an Entran EL, model ELFS-T3M-250N. It had a range of 250N and a sensitivity of 182·4mV at full scale with an excitation of 10Vdc. Thrust measurements were taken by sampling the load cell for one minute at each test point. Thrust measurements were taken for a range of engine speeds between 30,000rpm and 80,000rpm.

3.2 Spectroradiometer measurements

The spectroradiometer used was the CI Systems SR5000. It uses a filter wheel enabling radiation measurements to be taken between 1·296μm and 14·314μm. Measurements with the spectroradiometer were carried out at 45,000 rpm, 60,000 rpm and 80,000 rpm, at three positions of 20mm (0·43D), 170mm (3·6D) and 320mm (6·8D) behind the nozzle, viewing perpendicular to the jet flow, and two points viewing the jet obliquely — one at 10° and one at 45° to the flow. This is illustrated in Fig. 3. For each test case the spectroradiometer scanned the infra-red range from 1·296μm to 14·31μm split into 448 steps. Sixty full scans were carried out over a period of one minute for each position and each engine speed.

During initial running it was observed that the engine had an inherent low frequency pulsing of about 0·5Hz observed as a successive lengthening and shortening of the exhaust plume. The magnitude of this pulsing was approximately one nozzle diameter of plume length at engine start but reduced significantly (to one or two tenths of a nozzle diameter) once the engine had reached a stable operating temperature. The effect on the results was that the spectroradiometer effectively 'sees' a constantly varying length of plume when focussed on one point. To investigate this further, spectroradiometer measurements were taken with scan lengths from 0·5s to 16s. Irrespective of the length of the scans, the overall result was similar and so it was concluded that the engine pulsing did not appear to significantly affect the results. Sixty scans of one second duration were selected for data capture. Together with the spectroradiometer data, an infra-red camera operating in the 3–5μm band was used to view the plain and sixty degree nozzles with the engine at 60,000 rpm and 80,000 rpm.

3.3 Total pressure measurements

In order to further investigate the influence of the nozzle designs on the jet efflux, total pressure measurements were also made. A 4mm

https://doi.org/10.1017/S0001924000000580 Published online by Cambridge University Press



Figure 2. The Cobra turbo-jet engine on the test stand showing the data acquisition co-ordinate system.

outside diameter, 2mm inside diameter Pitot probe was attached to a computer-controlled traverse. The pressure transducer used was made by Micro and had a range of 0–20psig with a full scale output of 200mV. The pressure transducer was sampled for eight seconds at a frequency of 1kHz. The main pressure measurement test that was carried out was a plume transverse profile on an *x*-*y* grid of 100mm (2·1*D*) by 100 mm (2·1*D*) centred on the axis of the nozzle perpendicular to the flow, 20mm (0·43*D*) downstream of the nozzle exit plane. The measurement resolution was 5mm (0·11*D*) in the *x*-direction and 10mm (0·21*D*) in the *y*-direction (see Fig. 2). The engine was run at 60,000 rpm.

Additionally, stream-wise measurements of centreline total pressure for the plain and 60° nozzles were carried out with the engine at 45,000 rpm, 60,000rpm and 80,000rpm over a distance of 400mm (8·5*D*) with a 10mm (0·21*D*) resolution for the first 100mm (2·1*D*) and 20mm (0·43*D*) resolution for the remaining 300mm (6·4*D*). At the beginning and end of each set of pressure measurements an extra reading was taken in still air. An average of these two readings was then used to give the zero offset of the transducer.

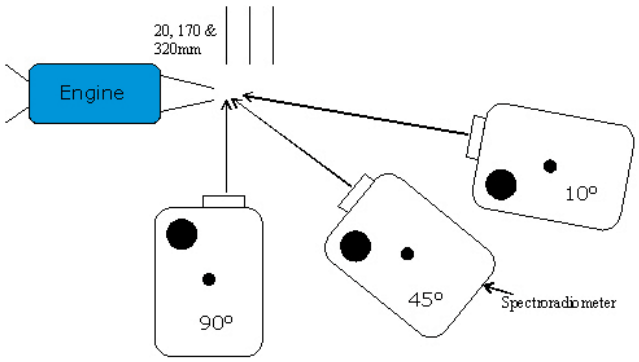


Figure 3. Schematic of the spectroradiometer measurements.

4.0 EXPERIMENTAL ERRORS

Before the results of the experiments are discussed it is necessary to explore the experimental errors that occurred.

4.1 Engine speed

The computer program used to read the engine speed could only resolve it to 250rpm hence, the operating speed could only be known to ±250rpm. Although the rpm could be resolved to this level the engine itself could not be held to a speed demand more accurately than ±1,000rpm.

4.2 Thrust measurements

Based on the non-linearity of the load cell, thrust measurements were accurate to ±1% of full scale (250N). The resolution of the load cell measurements was better than 0·01N.

4.3 Total pressure measurements

When collecting pressure data in the plume shear layer buffeting caused the Pitot probe to oscillate leading to a fluctuation in Pitot probe position during the reading. Each reading, however, was averaged from 8,000 samples, which should have damped out some of the effects. In the shear layer the magnitude of the oscillation was approximately ±10mm in a stream-wise direction, however, within the jet plume itself, the magnitude of the oscillations were observed to be significantly smaller (±2mm). The pressure transducer had an absolute error at full scale of no more than ±1%. The analogue-to-digital converter gave a pressure resolution of 4·2Pa.

5.0 RESULTS AND DISCUSSION

A quantitative assessment of the spectroradiometer and Pitot probe data is discussed below. The excessive vibration caused by the tabbed nozzle curtailed its test programme due to concern regarding potential engine damage.

5.1 Thrust measurements

It was anticipated that the increased exit area of the notched nozzles would cause a change in the performance characteristics of the engine when compared to the plain convergent design and so thrust measurements were made for each nozzle over a range of engine speeds. Fig. 4 shows the variation of thrust with engine speed for the plain convergent nozzle and each of the notched nozzles. A cubic best fit line has been added to each set of data. There is significant scatter in the data thought to be mainly due to variations in engine speed during data acquisition. Table 2 compares the manufacturer's quoted engine thrust performance with the calibration curves. These curves were extrapolated to give the theoretical thrust at 30,000rpm and 103,500rpm.

The calibration curves derived from the measured thrust data agree well with the manufacturer's quoted performance. The variation in engine thrust produced with the different installed nozzle types is within the experimental errors quoted previously, particularly at 80,000rpm where the majority of the spectroradiometer and Pitot probe data were taken.

https://doi.org/10.1017/S0001924000000580 Published online by Cambridge University Press

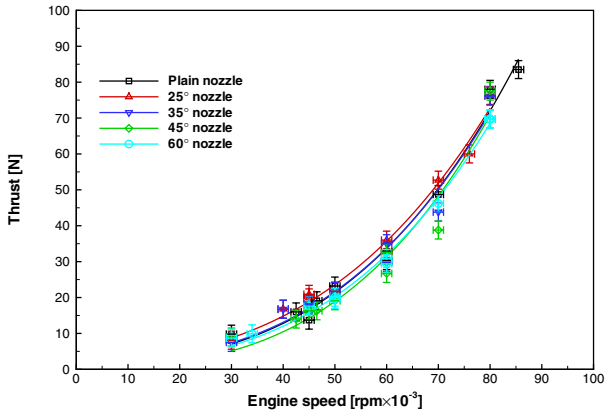


Figure 4. Measurement of thrust versus engine speed for the range of nozzles tested.

5.2 Infra-red imagery

Simultaneously with the spectroradiometer measurements (described below) a limited quantity of infrared imagery was recorded. Fig. 5 shows a comparison between the false-colour infra-red images recorded for the plain and 60° nozzles with the engine speed set to 60,000rpm. Colder regions (such as the background) appear blue transitioning through cyan, green, yellow, red, magenta and finally to white, which shows the hottest areas. The bell-mouth intake can just be made out as a green area at the front of the engine. The red band indicates the location of the compressor (the manufacturer's metallic logo appears as a yellow circle, c.f. Fig. 2), while the white region encompasses the combustion chamber, propelling nozzle and the hottest part of the jet plume. The imagery gives a qualitative indication of the reduction in infra-red signature when using the notched nozzle. The reduction in length of the hottest part of the jet plume is estimated at approximately 33% (from 6*D* to 4*D*).

Table 2
Comparison of extrapolations from the thrust calibration curves with manufacturer's data

		Thrust [N]				
Engine speed [rpm]	Manufacturer	Plain nozzle	25° nozzle	35° nozzle	45° nozzle	60° nozzle
30,000	6	7	9	7	5	7
60,000		34	36	34	31	32
80,000		72	73	71	71	69
103,500	150	147	144	145	149	140

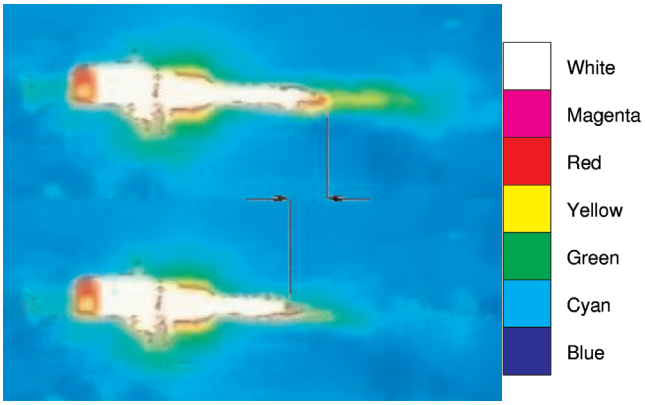


Figure 5. False-colour infra-red camera images of the jet plume at 60,000rpm engine speed: plain nozzle (top); 60° nozzle (bottom).

5.3 Spectroradiometer data

As mentioned previously the 3–5μm band is the wavelength spread of interest. Within this band the largest amount of radiation occurs at approximately 4.3μm, which is the wavelength of the radiation from CO_2 molecules. Taking spectroradiometer measurements is a problematic process due to the nature of the variance in the medium in which the data are collected. Since the absolute magnitude of the radiance from the CO_2 is relatively small then a small change in the level of the CO_2 in the exhaust gas can have a large effect on the measured radiance. The spectroradiometer works by comparing the subject data with reference data from a black body, ideally matched to the temperature of the subject. For the data presented, the black body temperature was set at 380°C (653K).

Figure 6 shows a typical set of spectroradiometer data measured normal to the plume axis, 20mm (0·43D) downstream of the nozzle exit plane with the engine at 80,000rpm. The configuration is representative of a side-on engagement scenario but it also most closely isolates the plume radiation from internal engine radiation. The plot shows the spectral radiance of the exhaust plume in the 3–5μm band *relative* to the reference black body. There is a clear spike for each of the nozzles tested at approximately 4·3μm, which correlates with the CO_2 in the plume. The plain nozzle returns the highest relative radiance (approximately 0·0045Wcm^{-2}μm^{-1}) with the 25° nozzle performing similarly. The 35° nozzle and 60° nozzle show a significant reduction in the relative spectral radiance with the 60° nozzle performing best of all. The notched nozzles appear to reduce the relative spectral radiance of the exhaust plume and generally, the broader the notches, the greater the reduction.

The lock-on range of an infra-red seeker is proportional to the power emitted by the target.

$$\text{Lock-on range} \propto \sqrt{\text{Target radiated power}} \quad \ldots \quad (1)$$

The 60° nozzle, therefore, gives a significant reduction in the lock-on range for a typical infra-red seeker.

Figure 7 shows similar data to that of Fig. 6 but in this case the spectroradiometer is focussed on a point 170mm (3·6*D*) downstream of the nozzle exit plane. The relative spectral radiance is significantly less at this downstream location. For this engine, the potential core is quite short (approximately 2·5*D*) and so at 3·6*D* downstream from the nozzle exit plane, viscous mixing has reduced the CO_2 levels in the plume and reduced the radiance. Again, the notched nozzles show a performance benefit over the plain convergent nozzle.

Figure 8 shows spectroradiometer data measured 10 degrees off axis from the nozzle centreline and focussed on the nozzle exit plane. The

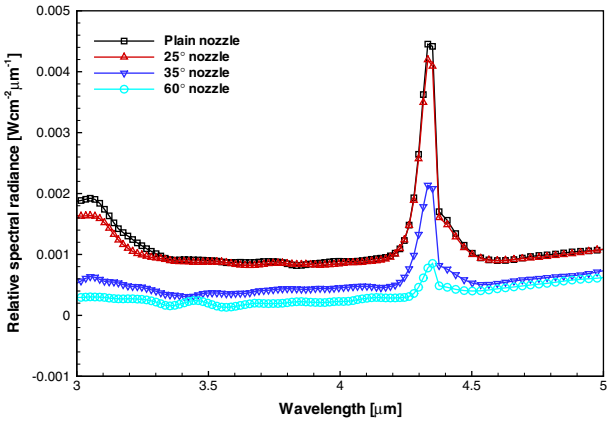


Figure 6. Relative spectral radiance in the 3–5μm band 20mm (0·43*D*) downstream, 80,000rpm.

https://doi.org/10.1017/S0001924000000580 Published online by Cambridge University Press

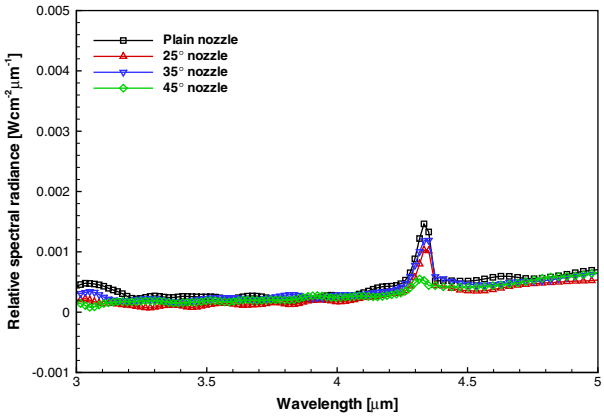


Figure 7. Relative spectral radiance in the 3–5μm band 170mm (3·6*D*) downstream, 80,000rpm.

engine speed was 60,000rpm in this case. Relative spectral radiance is similar in magnitude to that measured normal to the plume axis. Again, performance improvements are seen for the notched nozzles.

At 45 degrees off axis (Fig. 9) the notched nozzles give little or no reduction in relative spectral radiance. One of the important points to consider when taking readings at angles looking into the exit of the nozzle is that the spectroradiometer will not only see the exhaust plume but also the hot side wall of the nozzle and the reflected radiation from inside the engine.

5.4 Pressure distribution

To gain further insight into the effects the notched nozzles have on the exhaust plume fluid mechanics, the Pitot probe measurements will be examined. Figure 10 shows normalised nozzle centreline total pressure profiles as a function of streamwise distance. For both nozzle types shown, reducing the engine speed reduces the potential core length and increases the rate of decay of the exhaust plume. A comparison between the plain and 60° nozzles, however, shows that the latter promotes a reduction in the potential core length at the same engine speed. Additionally, the rate of decay of centreline total pressure is increased for the 60° nozzle. The changes observed in centreline total pressure suggests that the 60° nozzle is producing a more rapid mixing of the exhaust plume with the surrounding ambient air, presumably through the promotion of streamwise vorticity.

The area of the potential core as viewed from the side is directly proportional to the infra-red signature[9, 10]. For calculation purposes,

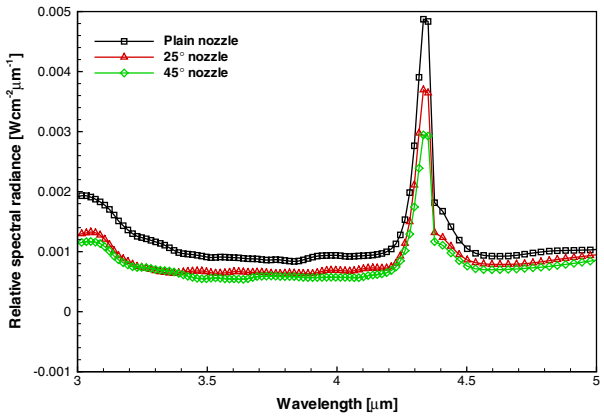


Figure 8. Relative spectral radiance in the 3–5μm band 10 degrees off axis, 60,000rpm.

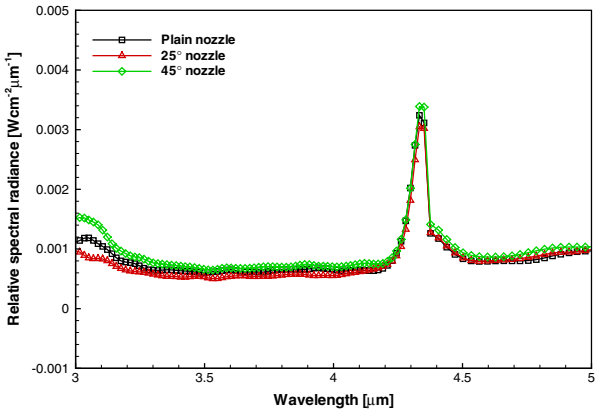


Figure 9. Relative spectral radiance in the 3–5μm band 45 degrees off axis, 80,000 rpm.

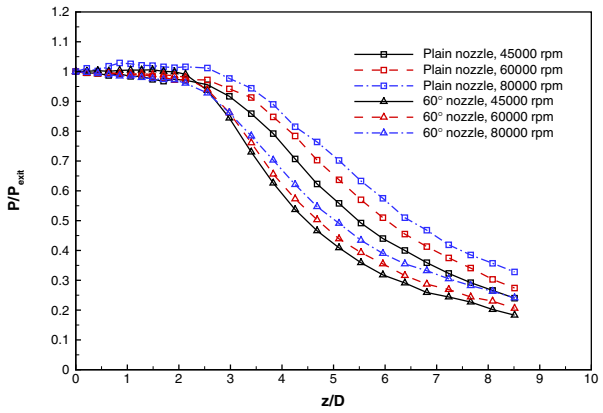


Figure 10. Streamwise centreline total pressure profiles for each of the nozzles tested.

it was assumed that the potential core ended when the total pressure had fallen to 95% of the nozzle exit value. The potential core areas for the plain and 60° nozzles are shown in Table 3 for three different engine speeds. The reduction in core area for the 60° nozzle varies from 4% at a high idle (45,000rpm) to 30% at 80,000rpm. Given that, within the accuracy of the acquired data, the variation of thrust with engine speed is the same for both nozzles, this translates into a real reduction in potential core length and, by implication, a reduction in infra-red signature, for no measureable performance penalty.

Contours to total pressure 20mm (0·43*D*) downstream of the nozzle exit plane are shown in Fig. 11 for the plain, 25°, 45° and 60° nozzles. The plain nozzle shows a reasonably axisymmetric contour given the measurement resolution described earlier. The notched nozzles, however, show a significant departure from

Table 3
Comparison of potential core areas for plain and 60° notched nozzles.

Engine speed [rpm]	Potential core Area [mm^2] Plain nozzle	60° nozzle	Difference [%]
45,000	2,891	2,773	4·1
60,000	3,196	2,773	13·2
80,000	3,713	2,562	31·0

https://doi.org/10.1017/S0001924000000580 Published online by Cambridge University Press

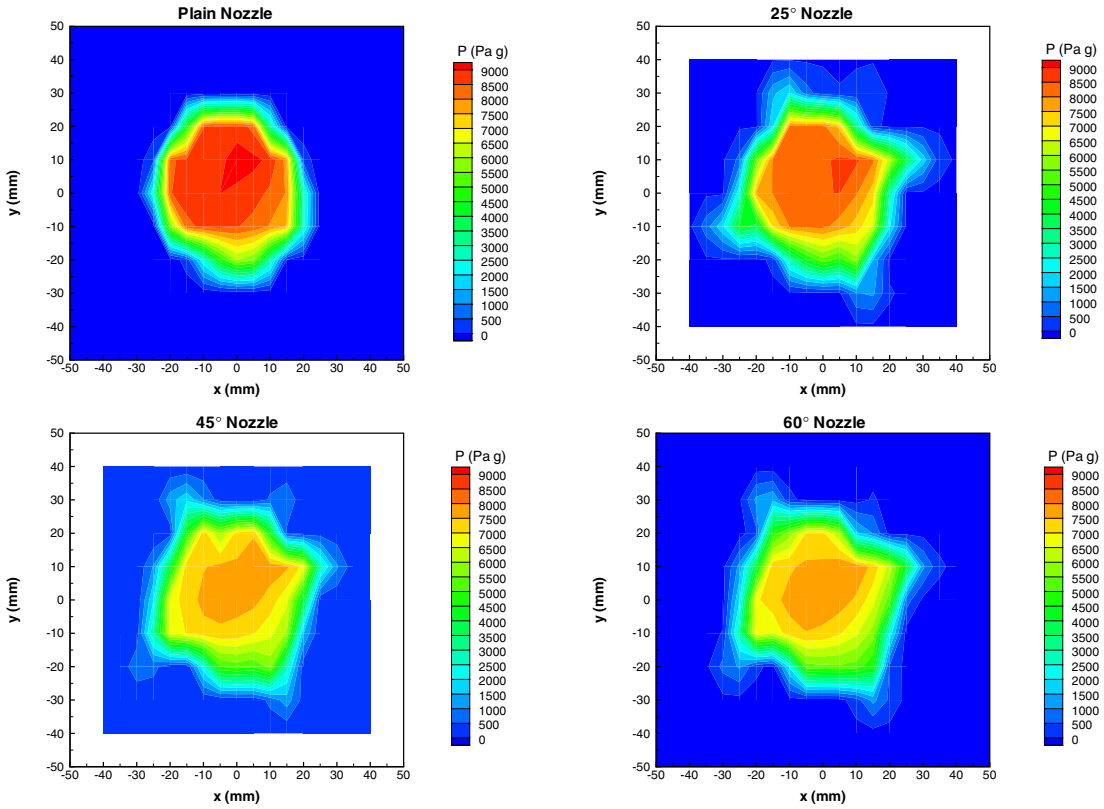


Figure 11. Contours of total pressure 20mm (0·43*D*) downstream of the nozzle exit plane.

axisymmetry and a reduced peak total pressure. The notched nozzles show four distinct 'lobes' in their pressure contour where the cut-outs have allowed the exhaust gas to spread radially. These 'lobes' have rotated anti-clockwise from the notch orientation along the *x* and y axes, possibly due to residual swirl in the exhaust flow.

6.0 CONCLUSIONS

A series of experiments has been conducted to investigate the potential reduction in infra-red signature of a centrifugal flow turbo-jet engine through the use of non-axisymmetric notched nozzles. The following conclusions are drawn from the data collected and experiences gained during testing.

- Correlation of engine thrust with engine rpm showed that, within the accuracy of the measurements, there was no thrust penalty associated with the notched nozzles.
- Infra-red imagery of the plain and 60° notched nozzles indicated that the latter reduced the length of the hottest part of the exhaust plume by approximately 33%.
- The spectroradiometer data shows a significant reduction in spectral radiance for the CO_2 wavelength of approximately 4·3μm when the notched nozzles are used. The 60° notched nozzle appeared to perform best in reducing the spectral radiance at this wavelength.
- Centreline total pressure measurements in the exhaust plume correlated well with the infra-red imagery in that a potential core length reduction of up to 30% could be achieved using the 60° notched nozzle.
- Total pressure contours recorded 20mm (0·43*D*) downstream of the nozzle exit plane suggest that the notched nozzles are promoting increased mixing through radial spreading of the jet possibly associated with increased streamwise vorticity (although the latter could not be confirmed).
- There were signs that the jet plumes being investigated were swirling.

REFERENCES

1. RAO, G.A. and MAHULIKAR, S.P. Integrated review of stealth technology and its role in airpower, *Aeronaut J,* December 2002, **106,** (1066), pp 629–641.
2. ROGERS, C.B. and PAREKH, D.E. Mixing enhancement by and noise characteristics of streamwise vortices in an air jet, *AIAA J,* March 1994, **32,** (3) pp 464–471.
3. SAMIMY, M., ZAMAN, K.B.M.Q. and REEDER M.F. Effect of tabs on the flow and noise field of an axisymmetric jet, *AIAA J,* April 1993, **31,** (4), pp 609–619.
4. SAMIMY, M. KIM, J.H. and CLANCY, P. Supersonic jet noise reduction and mixing enhancement through nozzle trailing edge modifications, 35th AIAA Aerospace Sciences Meeting and Exhibit, 6-9 January 1997, Reno, NV, Paper No 97-0146.
5. SAMIMY, M., KIM, J.H., and CLANCY, P. Mixing enhancement in supersonic jets via trailing edge modifications, 4th AIAA Shear Flow Control Conference, Snowmass, CO, 29 June-2 July 1997, Paper No 97-1877.
6. PANNU, S.S. and JOHANNESEN, N.H. The structure of jets from notched nozzles, *J Fluid Mechanics,* 1976, **74,** (3), pp 515–528.
7. SADDINGTON, A.J., KNOWLES, K. and WONG, R.Y.T. Numerical modelling of mixing in jets from castellated nozzles, *Aeronaut J*, December 2002, **106,** (1066), pp 643–652.
8. JAMES, D. *The Jet Cobra Users Manual.*
9. BANKEN, G.J. CORNETTE, W.M. and GLEASON, K.M. Investigation of infra-red characteristics of three generic nozzle concepts, 16th AIAA/SAE/ASME Joint Propulsion Conference, 30 June-2 July 1980, Hartford, CT, USA, Paper no AIAA-80-1160.
10. DECHER, R. Infra-red emissions from turbofans with high aspect ratio nozzles. *AIAA J,* December 1981, **18,** (12), pp 1025–1031.

https://doi.org/10.1017/S0001924000000580 Published online by Cambridge University Press